Science
AAAS

Bidirectional Control of Social Hierarchy by Synaptic Efficacy in Medial Prefrontal Cortex

Fei Wang, *et al.*

Science **334**, 693 (2011);
DOI: 10.1126/science.1209951

This copy is for your personal, non-commercial use only.

If you wish to distribute this article to others, you can order high-quality copies for your colleagues, clients, or customers by clicking here.

Permission to republish or repurpose articles or portions of articles can be obtained by following the guidelines here.

The following resources related to this article are available online at www.sciencemag.org (this infomation is current as of December 15, 2011):

Updated information and services, including high-resolution figures, can be found in the online version of this article at:
http://www.sciencemag.org/content/334/6056/693.full.html

Supporting Online Material can be found at:
http://www.sciencemag.org/content/suppl/2011/09/28/science.1209951.DC1.html

A list of selected additional articles on the Science Web sites **related to this article** can be found at:
http://www.sciencemag.org/content/334/6056/693.full.html#related

This article **cites 33 articles**, 8 of which can be accessed free:
http://www.sciencemag.org/content/334/6056/693.full.html#ref-list-1

This article has been **cited by** 1 articles hosted by HighWire Press; see:
http://www.sciencemag.org/content/334/6056/693.full.html#related-urls

This article appears in the following **subject collections:**
Neuroscience
http://www.sciencemag.org/cgi/collection/neuroscience

Downloaded from www.sciencemag.org on December 15, 2011

Science (print ISSN 0036-8075; online ISSN 1095-9203) is published weekly, except the last week in December, by the American Association for the Advancement of Science, 1200 New York Avenue NW, Washington, DC 20005. Copyright 2011 by the American Association for the Advancement of Science; all rights reserved. The title *Science* is a registered trademark of AAAS.

improve cerebellar phenotypes. It is encouraging that exercise and the accompanying increase in neuronal activity and metabolic demands do not seem to exacerbate the disease process in vulnerable neuronal populations, which may be important in a variety of neurodegenerative disorders.

References and Notes

1. H. T. Orr *et al.*, *Nat. Genet.* **4**, 221 (1993).
2. H. Y. Zoghbi, H. T. Orr, *J. Biol. Chem.* **284**, 7425 (2009).
3. C. W. Cotman, N. C. Berchtold, L.-A. Christie, *Trends Neurosci.* **30**, 464 (2007).
4. A. Chiò, G. Benzi, M. Dossena, R. Mutani, G. Mora, *Brain* **128**, 472 (2005).
5. D. J. Mahoney, C. Rodriguez, M. Devries, N. Yasuda, M. A. Tarnopolsky, *Muscle Nerve* **29**, 656 (2004).
6. K. Watase *et al.*, *Neuron* **34**, 905 (2002).
7. S. Astigarraga *et al.*, *EMBO J.* **26**, 668 (2007).
8. Y. C. Lam *et al.*, *Cell* **127**, 1335 (2006).
9. J. Crespo-Barreto, J. D. Fryer, C. A. Shaw, H. T. Orr, H. Y. Zoghbi, *PLoS Genet.* **6**, e1001021 (2010).
10. M. Kawamura-Saito *et al.*, *Hum. Mol. Genet.* **15**, 2125 (2006).
11. J. Lim *et al.*, *Nature* **452**, 713 (2008).
12. P. S. Thomas Jr. *et al.*, *Hum. Mol. Genet.* **15**, 2225 (2006).
13. J. M. Van Raamsdonk *et al.*, *Hum. Mol. Genet.* **14**, 1379 (2005).
14. D. V. Vaz *et al.*, *Clin. Rehabil.* **22**, 234 (2008).
15. W. Ilg *et al.*, *Neurology* **73**, 1823 (2009).

Acknowledgments: J.D.F. and H.Y.Z. conceived of the study and designed experiments. J.D.F., C.M.B., A.N.C., and Y.G. performed behavioral assays and provided input on analysis. J.D.F. and J.C.-B. performed molecular work and analysis. P.Y., H.K., and C.S. analyzed microarray data. J.D.F. and H.Y.Z. wrote the manuscript with input from J.C.-B, A.F., and H.T.O. We are grateful to G. Schuster for the generation of mutant mice and the members of the H.Y.Z. laboratory for comments and discussions on the manuscript. This research was supported by NIH grants NS27699, NS27699-20S1–ARRA, and HD24064 (Baylor College of Medicine–Intellectual and Developmental Disabilities Research Center) to H.Y.Z.; 1F32NS055545 to J.D.F.; and NS022920 and NS045667 to H.T.O. H.Y.Z. is an investigator with the Howard Hughes Medical Institute, holds a patent on SCA1 diagnostic testing, and is on the scientific advisory board of Pfizer Neuroscience Program.

Supporting Online Material

www.sciencemag.org/cgi/content/full/334/6056/690/DC1
Materials and Methods
Figs. S1 to S3
Tables S1 to S4
References (*16*–*18*)

15 August 2011; accepted 21 September 2011
10.1126/science.1212673

Bidirectional Control of Social Hierarchy by Synaptic Efficacy in Medial Prefrontal Cortex

Fei Wang,[1,2] Jun Zhu,[1] Hong Zhu,[1,2] Qi Zhang,[1] Zhanmin Lin,[1] Hailan Hu[1]*

Dominance hierarchy has a profound impact on animals' survival, health, and reproductive success, but its neural circuit mechanism is virtually unknown. We found that dominance ranking in mice is transitive, relatively stable, and highly correlates among multiple behavior measures. Recording from layer V pyramidal neurons of the medial prefrontal cortex (mPFC) showed higher strength of excitatory synaptic inputs in mice with higher ranking, as compared with their subordinate cage mates. Furthermore, molecular manipulations that resulted in an increase and decrease in the synaptic efficacy in dorsal mPFC neurons caused an upward and downward movement in the social rank, respectively. These results provide direct evidence for mPFC's involvement in social hierarchy and suggest that social rank is plastic and can be tuned by altering synaptic strength in mPFC pyramidal cells.

Dominance hierarchy is a fundamental organizing mechanism for most animal societies (*1*). The dominance status determines access to resources and profoundly affects survival, health, reproductive success, and multiple behaviors (*2*–*4*). Once established, the hierarchy rank is relatively stable and can minimize intense fights among group members (*5*). Dominance hierarchy emerges early in development and is present in children as young as 2 years old (*6*). Moreover, dominance has been linked to heritable traits in animals (*7*, *8*) and humans (*9*). The ubiquitous, inheritable nature and the early developmental emergence suggest that dominance hierarchy is encoded by innate neural mechanism (*10*). Yet, current understanding of the neural mechanisms associated with social hierarchy—the neural circuits underlying status-related behavioral differences and the mechanism for initiating changes in social status—is surprisingly limited.

[1]Institute of Neuroscience and State Key Laboratory of Neuroscience, Shanghai Institutes for Biological Sciences, Chinese Academy of Sciences, Shanghai 200031, China. [2]Graduate School of Chinese Academy of Sciences, Shanghai 200031, China.

*To whom correspondence should be addressed. E-mail: hailan@ion.ac.cn

To investigate the neural mechanisms underlying social hierarchy, a robust and reliable behavioral assay is essential. The tube test, in which one mouse forces its opponent out backward from a narrow tube—developed to measure the dominance tendency of mice (*11*) (Fig. 1A)—was previously used mostly for comparison between mice of different strains (*11*) or genotypes (*12*). To measure the hierarchical relation of animals within the same social group, we applied the tube test to cage groups of four male C57/BL6 mice, living together for at least 2 weeks. Mice were tested pair-wise using a round robin design, and the social rank was assessed on the basis of winning against the other three cage mates (Fig. 1, A and D). We validated the tube test to be a reliable measure of dominance ranking by the following three criteria:

1) Transitivity—when mouse A is more dominant over B and B more dominant over C, then A should be dominant over C (Fig. 1B). We analyzed the relation of any three mice from a cage group; rank was transitive in 95% (251 out of 264) cases (Fig. 1B). Consistent with this high transitivity, in 89% (78 out of 88) of the trials, a four-mouse group adopted a linear social diagram among the four possible combinations (Fig. 1C).

2) Stability over time (*2*). For stability evaluation, rank was measured daily for 7 days (Fig. 1, D and E). Mice adopted the same rank position as the previous day in 59% (127 out of 216) of the comparisons. Having a reward for taking the tube test (see Methods) did not affect the linearity or stability of the rank (Fig. 1C and fig. S1A). It was noteworthy that the time spent in the tube was significantly shorter when the mouse of the lowest rank (rank-4) was involved or as rank distance increased (Fig. 1F). Moreover, rank did not correlate with either the weight (when weight difference is below 15%) ($P = 0.96$, one-way analysis of variance) (fig. S1B) or the locomotive activity in the open field ($P = 0.41$) (fig. S1C).

3) Consistency with results of other dominance measures. To rule out factors unrelated to dominance, e.g., sensorimotor capacity, learning ability, and persistence, we compared the tube test results with those obtained by five additional dominance assays. First, in the visible burrow system (VBS), where food and water are relatively difficult to access and weight change reflects dominance (*13*), the tube-test ranks correlated linearly with weight changes (Fig. 2A and fig. S2A). Second, tube-test ranks also linearly correlated with the ranks by the agonistic behavior test, in which dominance is determined by scoring agonistic behaviors in a novel context (Fig. 2B and fig. S2B). Third, in the barber assay where the most dominant mouse barbers the whiskers of its cage mates ("Dalila effect") (*12*, *14*), the barber mouse was ranked first by the tube test in six of seven cages (Fig. 2C). Fourth, in the urine-marking assay, where dominant mice mark larger territories than subordinate ones (*15*), we found 71% (30 out of 42) consistency with the tube-test result (Fig. 2D). Finally, in the test of ultrasonic vocalization toward females in which dominant males emit more 50- to 70-kHz ultrasonic courtship songs (*16*), we found rank-1 mice in the tube test emitted markedly more ultrasounds toward a female than mice of lower ranks in 9 out of 10 cages (Fig. 2E and fig. S2C). In addition, dominance ranking significantly correlated among these five tests themselves (fig. S2). Although the reliability and validity of each assay in measuring the dominance behavior may be debatable

Downloaded from www.sciencemag.org on December 15, 2011

or context-dependent (*5*, *17*), the high consistency of ranking results from these multiple assays strongly supports the notion that dominance is a common dependable variable underlying a variety of behaviors that use different sensorimotor skills (fig. S3).

Where and how is the hierarchical information encoded in the brain? Functional brain imaging studies in humans have implicated the dorsolateral prefrontal cortex (dlPFC) and medial prefrontal cortex (mPFC) in dominance hierarchy–related behaviors (*18*, *19*). The functional homo-

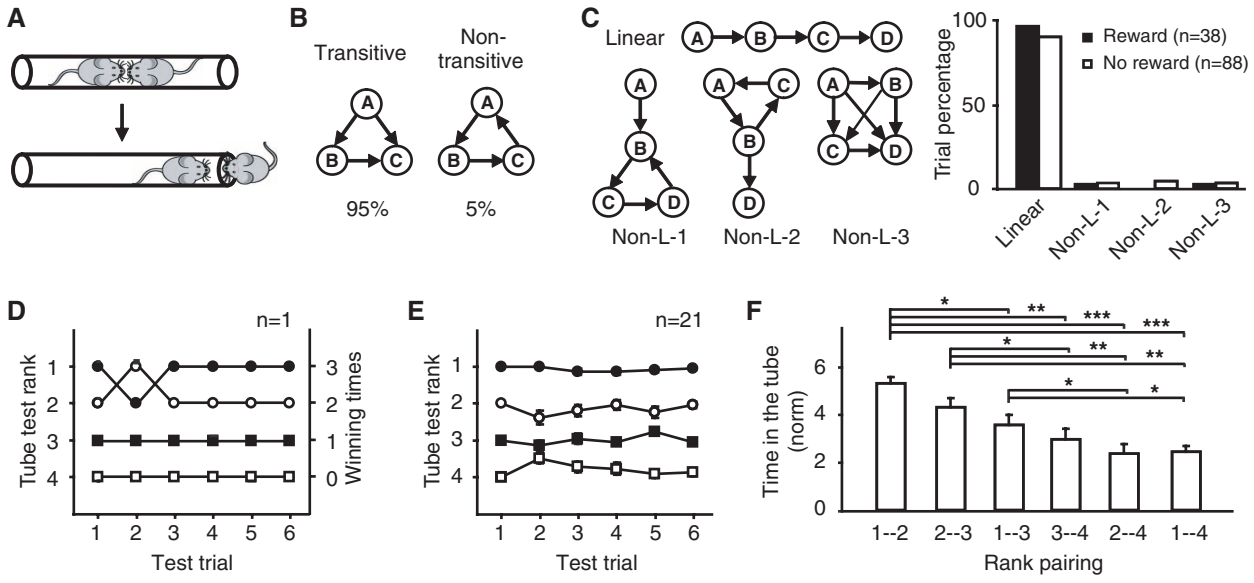

Fig. 1. Tube-test ranking for social hierarchy. (**A**) Schematic of the tube test. (**B**) Illustration of a transitive and a nontransitive relation (n = 264 cases). (**C**) Four possible social diagrams for a cage of four mice and the percentage of each diagram observed (n = number of cages). Non-L: non-linear. Histograms: Percentages of all cases that conformed to various social diagrams in the reward and nonreward conditions (see Materials and Methods). (**D**) Example of the rank positions of one cage of mice tested daily over 6 days. (**E**) Summary graph for 21 cages measured. The average rank positions of animals belonging to each rank group from the previous day were calculated. (**F**) Normalized time spent in the tube encountering for the six pairing conditions (n = 10 cages), e.g., 1–2 stands for rank-1 against rank-2. Wilson rank-sum test (*P < 0.05; **P < 0.01; ***P < 0.001). Error bars, SEM.

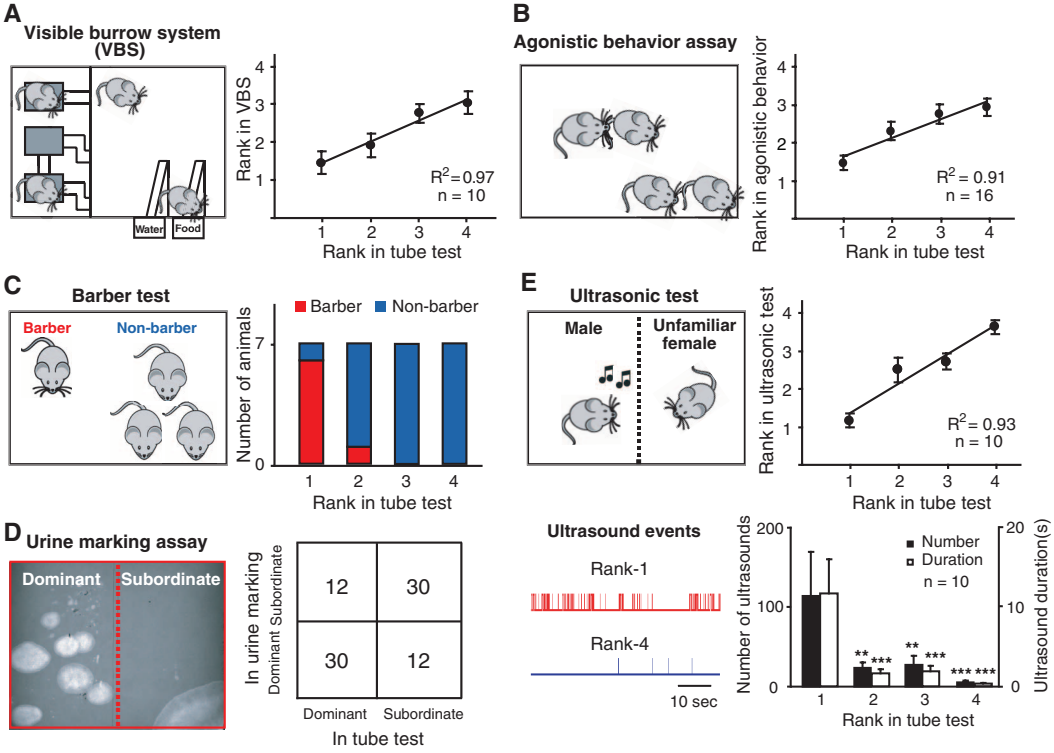

Fig. 2. Comparison of the tube test with five other dominance tests. (**A** to **E**) (Left) schematics of each test. (A) (Right) Average weight-change ranks in VBS plotted against the tube-test ranks. P = 0.0003, Fisher's exact test, same for (B) to (D). For (A), (B), and (E), n = number of cages. (B) The agonistic behavior score was calculated by subtracting the number of offensive behaviors from that of defensive behaviors during a 20-min period in a novel cage. (Right) Average ranks in agonistic behavior assay plotted against the tube-test ranks. P = 0.003. (C) (Right) Number of animals at each tube-test rank position from all the barber and nonbarber mice. P = 0.02. (D) (Left) Representative picture of the urine-marking patterns of a rank-1 to -4 mice pair as revealed by ultraviolet light. (Right) Contingency table showing number of animals in each category. n = 42 pairs from eight cage groups. P = 0.003. (E) (Top right) Average ranks in the ultrasound test against the tube-test ranks. $P = 2 \times 10^{-7}$. (Bottom left) Example traces of the ultrasound emitted by a pair of rank-1 and rank-4 male mice when encountering a female. (Bottom right) Summary graph of the number and duration of ultrasounds evoked by mice of each rank position. The P value is obtained by two-tailed Student's t test on natural log–transformed data in comparison with rank-1. **P < 0.01; ***P < 0.001. Error bars, SEM.

Downloaded from www.sciencemag.org on December 15, 2011

log of these regions in rodents is the dorsal mPFC, including the anterior cingulate cortex (AC) and the prelimbic cortex (PL) (Fig. 3A) (*20*). Moreover, mPFC lesion lowered the social rank in rats (*21*). Therefore, we investigated potential differences in the synaptic properties in this region between dominant and subordinate mice. Acute brain slices containing mPFC were made from rank-1 and rank-4 mice, and miniature excitatory synaptic currents (mEPSCs) mediated by the α-amino-3-hydroxy-5-methyl-4-isoxazolepropionic acid (AMPA) subtype of glutamate receptors were measured by whole-cell recording from layer V pyramidal neurons, the primary mPFC output neurons (Fig. 3B). The amplitudes, but not the frequency, of mEPSCs were significantly larger in rank-1 than rank-4 mice of the same cage group ($P < 0.0001$, Kolmogorov-Smirnov two-sample test) (Fig. 3, C and D). The difference was significant for each of the five pairs of mice recorded (Fig. 3E). These results indicate dominant mice have a higher excitatory synaptic strength in layer V pyramidal neurons than their subordinates, which could result in stronger output of these excitatory neurons to other brain regions. Consistently, dominant mice exhibited significantly higher number of c-Fos–positive neurons in the PL region of mPFC after the tube test (Fig. 3, F and G).

To determine whether the difference in mPFC synaptic efficacy could contribute to the rank status, we manipulated the function of excitatory synapses in dorsal mPFC using a *Sindbis* virus–based in vivo recombinant DNA–delivery technique (*22*–*24*) (Fig. 4A). Small guanosine triphosphatases Ras and Rap potentiate and depress AMPA receptor–mediated transmission, respectively, in the hippocampus by regulating synaptic trafficking of AMPA receptors (*25*). We verified these effects in the mPFC neurons in vivo by localized mPFC injection of Ras- or Rap-expressing *Sindbis* viruses and whole-cell recording of injected neurons (Fig. 4B). *Sindbis* virus preferentially infects pyramidal neurons (fig. S4), and the basic electrophysiological properties of infected neurons, including the input resistance and leak current, were indistinguishable from those of uninfected neurons within 48 hours of infection (fig. S4, see also SOM text note 1). At 12 to 24 hours postinfection, neurons infected with Ras virus had higher amplitudes of AMPA receptor–mediated EPSCs (179 ± 24% of controls, $P = 0.0093$, Wilcoxon signed rank test), in comparison with neighboring uninfected control cells (Fig. 4, B and E, and fig. S5A), whereas Rap-expressing neurons had lower EPSC amplitudes (Fig. 4E and fig. S5B, 71 ± 9% of controls, $P = 0.025$). The behavioral consequences of these synaptic manipulations were further assessed by bilateral high-titer viral injection into the dorsal mPFC of one mouse from each cage group with stable ranks (persisting for at least four continuous daily trials before the injection) (fig. S7). Mice infected with Ras virus moved upward in the rank, starting as early as 12 hours after viral injection (Fig. 4, F and G, and fig. S8A). In contrast, mice infected with Rap virus moved downward in the rank (Fig. 4, F and G, and fig. S8B). Infection of virus expressing green fluorescent protein (GFP) alone did not result in any rank shift (Fig. 4, F and G, and fig. S8E).

As the synaptic effect of Ras may involve both pre- and postsynaptic changes (*25*, *26*) and Ras-induced synaptic potentiation was relatively transient (<3 days) (fig. S6), we then manipulated the AMPA receptor–mediated transmission more specifically by using constructs that express either the AMPA receptor subunit GluR4, which undergoes synaptic delivery and increases synaptic transmission under basal conditions (*27*, *28*) (see also SOM text note 2), or the C terminus of GluR4 (R4Ct), which can block synaptic trafficking of AMPA receptors (*27*) (see also SOM text note 3). Recording in acute mPFC slices from virus-infected mice revealed that viral expression of GluR4 potentiated (173 ± 22% of controls, $P = 0.01$), whereas R4Ct depressed (24 ± 2% of controls, $P = 0.0006$), AMPA-EPSCs in mPFC (Fig. 4, C to E, and fig. S5). Correspondingly, GluR4 increased, whereas R4Ct decreased the tube-test rank of injected animals (Fig. 4, F to G, and fig. S8). Analysis of the viral infection sites reveals that the rank change correlated best with the infection rates in the PL region (fig. S7). Injection of the same amount of R4Ct virus into the M1 motor cortex had no effect on the rank (Fig. 4G

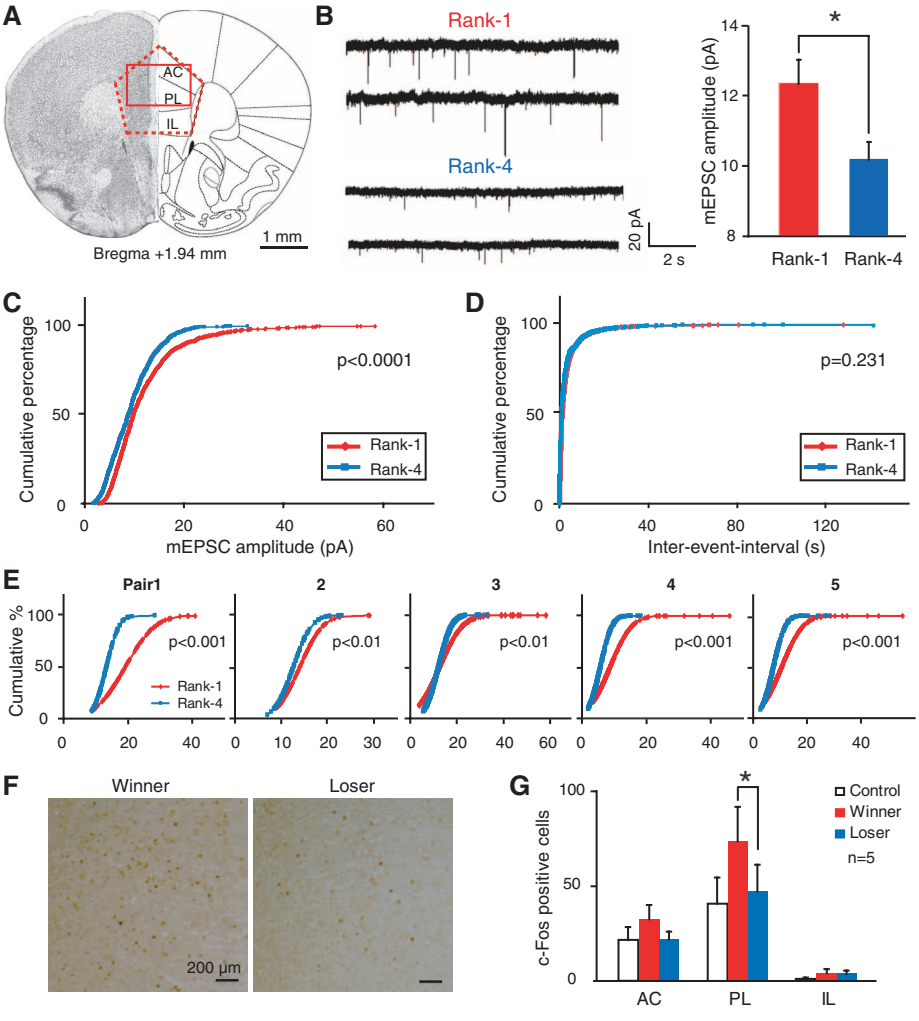

Fig. 3. Dominant mice have larger synaptic strength than the subordinate ones. (**A**) Schematic diagram of mPFC, as outlined by the red dashed lines. The smaller red box indicates the positions of the recordings made, mostly in AC and PL. (**B**) (Left) Representative traces of mEPSCs from mPFC layer V pyramidal neurons of a pair of rank-1 and rank-4 mice. (Right) Summary of the results from 60 neurons of five pairs of mice (12 neurons from each animal). The *P* value is obtained by two-tailed Student's *t* test on log-transformed data. (**C**) Cumulative distribution of mEPSC amplitudes of all 60 neurons. (**D**) Cumulative distribution of mEPSC inter event intervals (equal to 1 per frequency). (**E**) Cumulative distribution of mEPSC amplitudes from the 12 neurons of each individual pair of animals. (**F**) Representative images of PL slices from a winner and loser mouse stained for c-Fos 120 min after 5 rounds of tube test. (**G**) Average c-Fos–positive cell counts per 30-μm-thick slice. Two-tailed Student's *t* test. *$P < 0.05$. Error bars, SEM.

Downloaded from www.sciencemag.org on December 15, 2011

and fig. S9), which indicated that the effect is mPFC-specific.

To confirm that viral manipulations in mPFC affected dominance instead of other variables that could alter tube-test behavior (fig. S3), we performed an additional dominance measure, the ultrasonic vocalization test. When tested for ultrasound vocalizations toward a female, low-rank mice injected with GluR4-expressing virus displayed a significant increase, whereas high-rank mice injected with R4Ct-expressing virus showed a marked decrease in both the frequency and duration of ultrasound production at 36 to 60 hours after viral injection (Fig. 4H and fig. S10), resulting in a bidirectional shift in ultrasonic test rank (Fig. 4I and fig. S10).

Here, we established that the tube test is a simple and reliable method that provides hierarchical ranking of social groups in mice. Using this and other dominance measures, we identified the mPFC circuitry, in particular the dorsal mPFC, as a neural substrate for dominance hierarchy. The bidirectional modulation suggests that the effect of mPFC synaptic efficacy on dominance is specific and unlikely to be due to secondary effects.

How could mPFC contribute to the determination of social status? Social hierarchy behavior depends on a collection of cognitive traits involving recognition of social status, learning of social norms, and detection of violation of social norms (*10*). mPFC has been explicitly implicated in social cognition (*29*). Through its projections

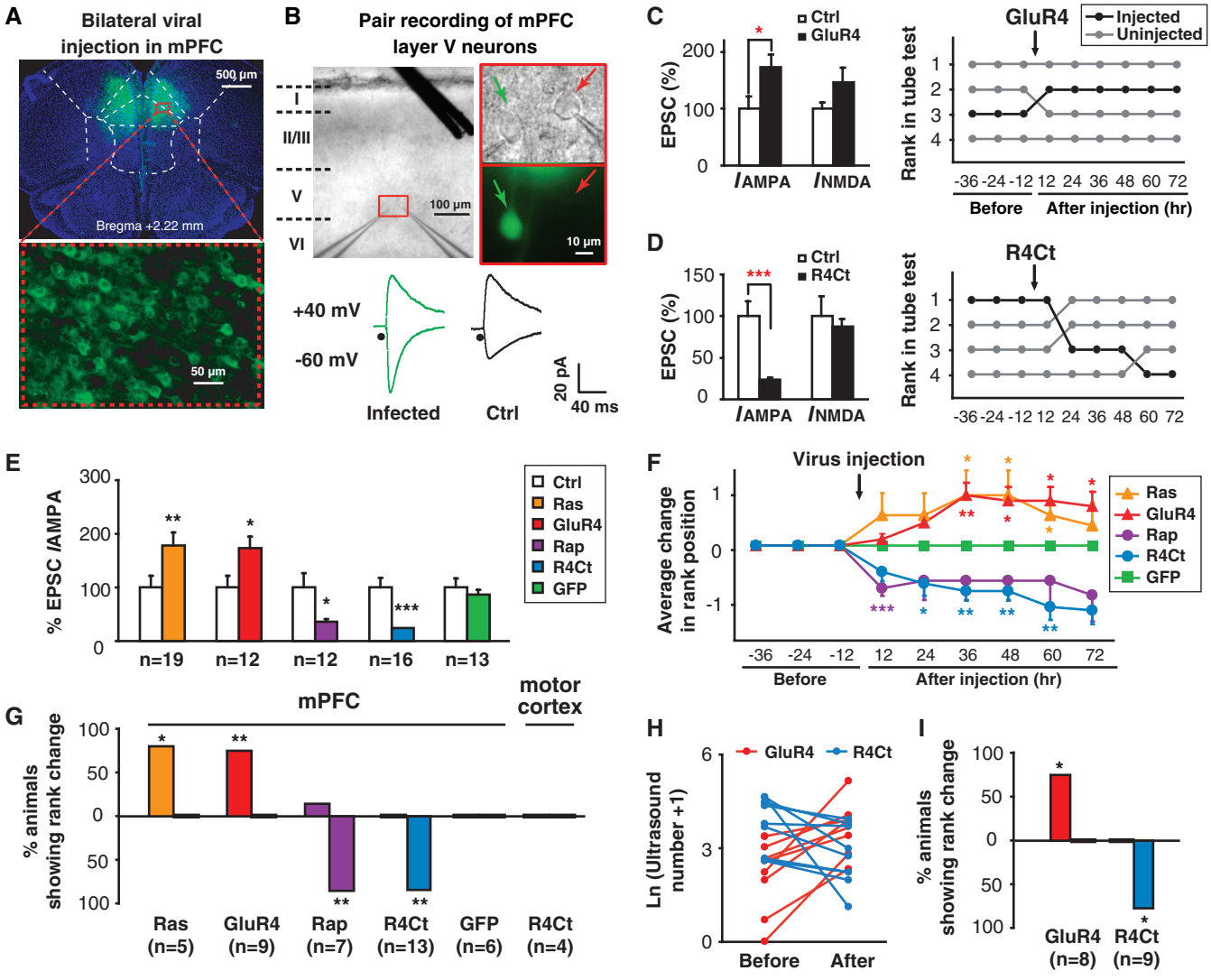

Fig. 4. Modulations of mPFC synaptic efficacy caused bidirectional shift of hierarchical rank. (**A**) Example of GFP-GluR4 virus injection sites (counterstained with Hoechst). White dashed lines outline the mPFC. (**B**) Simultaneous whole-cell recording of EPSCs from a pair of layer V pyramidal neurons while layer II/III was stimulated. (Top left) Illustration of the recording configuration. (Top right) Patching of a pair of infected (by GFP-Ras) and uninfected mPFC neurons under transmitted and fluorescent light microscopy. (Bottom) Example of evoked EPSC recorded at −60 and +40 mV from a neuron pair. Stimulation artifacts are marked by filled circles. (**C** and **D**) Effects of virus expressing GFP-GluR4 (C) and red FP (RFP)–R4Ct (D) on the AMPA receptor– and *N*-methyl-D-aspartate (NMDA) receptor–mediated EPSCs (left) and the tube-test rank dynamics of a four-mouse group (right). Arrowhead indicates the injection at 0 hours time point. (**E** and **F**) Summary of effects on AMPA receptor–mediated EPSCs (E) and tube-test rank (F) as induced by injection of each viral construct. *n* in (F) is the same as in (G). (**G**) Summary of percentage of animals showing rank increase (left upward column) or decrease (right downward column) in the tube test. (**H**) Natural log–transformed number of ultrasonic vocalization events toward a female before and after viral injection. Natural log transformation was taken to normalize the data and reduce the data span. Each line represents data from one mouse. (**I**) Summary of percentage of mice showing rank increase or decrease in ultrasound test induced by GluR4 and R4Ct viruses. (C) to (F) and (I) Wilcoxon signed rank test, in comparison with neighboring noninjected control neurons (C) to (E) or with rank change of animals injected with GFP-expressing virus (F) or noninjected animals (I). (G) Fisher's exact test, compared with GFP-injected animals. $^{*}P < 0.05$; $^{**}P < 0.01$; $^{***}P < 0.001$. Error bars, SEM.

Downloaded from www.sciencemag.org on December 15, 2011

to regions such as dorsal raphe, ventral tegmental area, hypothalamus, and amygdala, mPFC exerts top-down controls on serotonin and dopamine release, endocrine function, and fear response. All of these could contribute to key features of the dominance behaviors, including aggressiveness, stress responsiveness, and fearfulness. It will be of interest to determine which of these mPFC downstream circuits are specifically involved in setting the dominance hierarchy and to investigate how the dominance rank is initiated and maintained by differential neuronal activities in these circuits. Likewise, it will also be important to understand how the behavioral specificity of mPFC is generated by distinct upstream inputs, given the multiple functions that mPFC has been implicated in [reviewed by (*30*) and, recently, (*31*–*34*)]. The identification of a neural substrate of dominance hierarchy should provide new insights into the coding of a fundamental social behavior in the mammalian nervous system.

References and Notes

1. E. O. Wilson, *Sociobiology: The New Synthesis* (Harvard Univ. Press, Cambridge, MA, 1975).
2. I. S. Bernstein, *Behav. Brain Sci.* **4**, 419 (1981).
3. R. M. Sapolsky, *Science* **308**, 648 (2005).
4. S. R. Yeh, R. A. Fricke, D. H. Edwards, *Science* **271**, 366 (1996).
5. C. Drews, *Behaviour* **125**, 283 (1993).
6. D. G. Frankel, T. Arbel, *Int. J. Behav. Dev.* **3**, 287 (1980).
7. J. Masur, M. A. Benedito, *Nature* **249**, 284 (1974).
8. D. A. Dewsbury, *Anim. Behav.* **39**, 284 (1990).
9. A. Mehrabian, *Curr. Psychol.* **14**, 261 (1996).
10. D. D. Cummins, *Synthese* **122**, 3 (2000).
11. G. Lindzey, H. Winston, M. Manosevitz, *Nature* **191**, 474 (1961).
12. A. S. Garfield *et al.*, *Nature* **469**, 534 (2011).
13. H. Arakawa, D. C. Blanchard, R. J. Blanchard, *Behav. Brain Res.* **176**, 27 (2007).
14. S. Y. Long, *Anim. Behav.* **20**, 10 (1972).
15. L. C. Drickamer, *Behav. Processes* **53**, 113 (2001).
16. J. Nyby, G. A. Dizinno, G. Whitney, *Behav. Biol.* **18**, 285 (1976).
17. D. Benton, J. C. Dalrymplealford, P. F. Brain, *Anim. Behav.* **28**, 1274 (1980).
18. C. F. Zink *et al.*, *Neuron* **58**, 273 (2008).
19. J. Y. Chiao, *Curr. Opin. Neurobiol.* **20**, 803 (2010).
20. H. B. Uylings, H. J. Groenewegen, B. Kolb, *Behav. Brain Res.* **146**, 3 (2003).
21. R. R. Holson, *Physiol. Behav.* **37**, 239 (1986).
22. H. Marie, W. Morishita, X. Yu, N. Calakos, R. C. Malenka, *Neuron* **45**, 741 (2005).
23. S. G. McCormack, R. L. Stornetta, J. J. Zhu, *Neuron* **50**, 75 (2006).
24. H. L. Hu *et al.*, *J. Neurosci.* **28**, 7847 (2008).
25. J. J. Zhu, Y. Qin, M. Zhao, L. Van Aelst, R. Malinow, *Cell* **110**, 443 (2002).
26. S. A. Kushner *et al.*, *J. Neurosci.* **25**, 9721 (2005).
27. J. J. Zhu, J. A. Esteban, Y. Hayashi, R. Malinow, *Nat. Neurosci.* **3**, 1098 (2000).
28. J. J. Zhu, *J. Neurosci.* **29**, 6320 (2009).
29. D. M. Amodio, C. D. Frith, *Nat. Rev. Neurosci.* **7**, 268 (2006).
30. R. P. Vertes, *Synapse* **51**, 32 (2004).
31. H. E. Covington 3rd *et al.*, *J. Neurosci.* **30**, 16082 (2010).
32. O. Yizhar *et al.*, *Nature* **477**, 171 (2011).
33. K. Guillem *et al.*, *Science* **333**, 888 (2011).
34. D. Tse *et al.*, *Science* **333**, 891 (2011).

Acknowledgments: We thank J. Zhu for the gifts of pSindbis GluR4 and R4Ct constructs and discussion on GluR4; R. Malinow for support of the initial exploration of the tube test in his laboratory; M. Poo, H. Kessels, J. Feldman, and R. Sapolsky for discussion and critical reading of the manuscript; J. Yan for help with statistics; B. Lu for the idea of agonistic behavior test; B. Zhang, K. Zhang, and M. Streets for technical help; Y. Yanagawa for the Gad67-GFP mouse; and X. Yu for ultrasound equipment. The work was supported by Chinese 973 Program (2011CBA00400), Projects of the Scientific Research Foundation, the Hundreds of Talents Program, and the Shanghai Pujiang Talent Program to H.H. Author contributions: F.W. performed most experiments. J.Z. participated in the behavioral and viral injection experiments. F.W., J.Z., and H.H. analyzed data and prepared the figures. H.Z, Q.Z., and Z.L. assisted in experiments. H.H. designed the study and wrote the manuscript.

Supporting Online Material

www.sciencemag.org/cgi/content/full/science.1209951/DC1
Materials and Methods
SOM Text
Figs. S1 to S10
References

17 June 2011; accepted 9 September 2011
Published online 29 September 2011;
10.1126/science.1209951

Social Network Size Affects Neural Circuits in Macaques

J. Sallet,[1,2]*† R. B. Mars,[1,2]* M. P. Noonan,[1,2]* J. L. Andersson,[2] J. X. O'Reilly,[2] S. Jbabdi,[2] P. L. Croxson,[1,3] M. Jenkinson,[2] K. L. Miller,[2] M. F. S. Rushworth[1,2]

It has been suggested that variation in brain structure correlates with the sizes of individuals' social networks. Whether variation in social network size causes variation in brain structure, however, is unknown. To address this question, we neuroimaged 23 monkeys that had been living in social groups set to different sizes. Subject comparison revealed that living in larger groups caused increases in gray matter in mid-superior temporal sulcus and rostral prefrontal cortex and increased coupling of activity in frontal and temporal cortex. Social network size, therefore, contributes to changes both in brain structure and function. The changes have potential implications for an animal's success in a social context; gray matter differences in similar areas were also correlated with each animal's dominance within its social network.

The evolution of primate brains is thought to be associated with the demands of living in a complex social environment (*1*). Recent evidence shows that differences in brain structure correlate with variation in individuals' social network size (*2*); some brain structures are larger in people in regular contact with a larger number of relatives, friends, and colleagues. However, the direction of cause and effect underlying this phenomenon is unknown. Although this issue has not been directly investigated, sensorimotor experience is known to lead to brain structural changes even during adulthood (*3*, *4*). For instance, learning to use a tool increases gray matter density in the intraparietal sulcus (IPS), caudal superior temporal sulcus (STS), and somatosensory cortex in the rhesus macaque (*Macaca mulatta*) (*3*). Here, we exploit the pseudo-randomized assignment of individual animals to social groups in a research colony (*5*) to demonstrate that variation in young adult rhesus macaques' social environments changes structure and function in a distributed neural circuit centered on mid-STS, anterior cingulate cortex (ACC), and rostral prefrontal cortex (rPFC).

First, we conducted a deformation-based morphometric (DBM) analysis (*6*) of magnetic resonance imaging (MRI) scans of brain structure from 23 young adult [4.33 ± 0.52 years (mean ± SD)] monkeys (14 males) (*5*). Scanned animals were drawn from 34 animals from different groups within a research colony. The animals were housed in groups of between one and seven individuals. We considered the number of housemates of each monkey as a measure of social network size.

The organization of monkeys into groups was not randomized in a conventional sense but instead depended on factors that were independent of social characteristics; these included the requirements of independent programs of neuroscientific research and veterinary considerations [full details of housing arrangements are provided (*5*)]. A true randomization of animals would have been virtually impossible given numerous considerations, including the constraints imposed by the licensing of experimental procedures, the cost of such a project, and the potential for disruption to other research programs. While some unobserved variables might have contributed to the outcomes we report, group assignment was not carried out on the basis of social character-

[1]Department of Experimental Psychology, University of Oxford, Oxford OX1 3UD, UK. [2]Oxford Centre for Functional Magnetic Resonance Imaging of the Brain (FMRIB), University of Oxford, Oxford OX1 3UD, UK. [3]Icahn Medical Institute, Mount Sinai School of Medicine, New York, NY 10029, USA.

*These authors contributed equally to this work.
†To whom correspondence should be addressed. E-mail: jerome.sallet@psy.ox.ac.uk

Downloaded from www.sciencemag.org on December 15, 2011